J. Fluid Mech. (2009), *vol.* 626, *pp.* 263–289.
doi:10.1017/S0022112009005874 Printed in the United Kingdom

On the thermocapillary motion of partially engulfed compound drops

L. ROSENFELD, O. M. LAVRENTEVA AND A. NIR†

Chemical Engineering Department, Technion, Haifa 32000, Israel

(Received 7 April 2008 and in revised form 23 December 2008)

In this work the thermocapillary-induced motion of partially engulfed compound drops is considered. This phenomenon occurs in many natural and technological processes in which heat is exchanged between such hybrid drops and the medium around them through the interfaces. Two types of thermal fields and the resulting motions are studied; flow induced by an external temperature gradient and spontaneous thermocapillary motion. For the first flow type, it was found that, in general, the motion is induced in the direction of the temperature gradient. However, under certain physical conditions and drops' configuration a motion against the temperature gradient may be observed. In the second case, spontaneous thermocapillary motion, the compound drop moves due to surface tension gradients which result from the geometric non-uniformity of the system. Results are presented for several parameters such as configuration of the compound drop, viscosity, thermal conductivity ratio, the dependence of the various interfacial tensions on temperature and the volume ratio of the phases within the drop.

1. Introduction

Compound drops are comprised of two or more immiscible phases. They occur in various natural and technological processes such as melting of ice particles in the atmosphere, direct contact heat exchange, rapid evaporation of drops in a superheated liquid, liquid membranes and liquid bi-layers, etc. Torza & Mason (1970) were the first to study a static two fluid drop configuration as well as the dynamics of engulfing and coalescence. They showed that the occurrence of a particular type of configuration (complete engulfment, partial engulfment or non-engulfment) was determined solely by the values of surface tension between the three phases. In the case of partial engulfment, the three interfaces at equilibrium are segments of spheres and the resulting configuration of the aggregate depends on the volumes of the two droplets (see figure 1). Vuong & Sadhal (1989*a*) have studied the fluid dynamics associated with a compound drop consisting of a vapour phase partially surrounded by its own liquid immersed in another immiscible liquid. The exact solution of this compound drop system, describing the growth and translation of an axisymmetric liquid–vapour drop, was found. Oğuz (1987) has studied the case of hydrodynamics of partially engulfed drops and bubbles. The authors in these studies used the toroidal coordinate system which is highly useful in the treatment of fluid flow problems involving lens-shaped axisymmetric bodies as was shown by Payne & Pell (1960). A review on the subject of the dynamics of compound drops is given in Johnson & Sadhal (1985).

† Email address for correspondence: avinir@tx.technion.ac.il

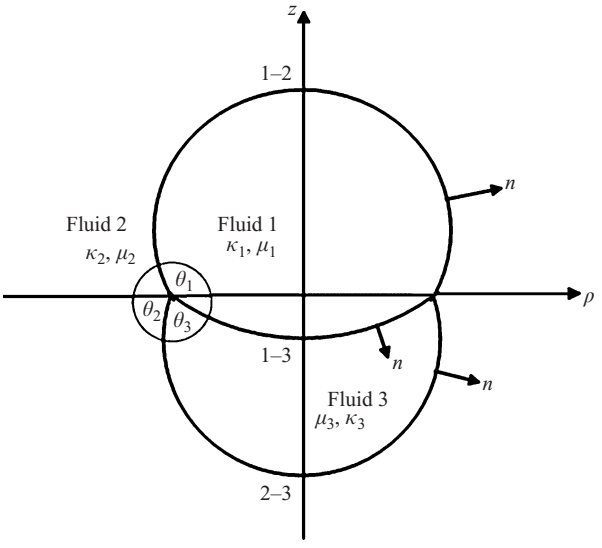

FIGURE 1. Configuration of a partially engulfed fluid–fluid compound drop.

In many processes involving compound drops, a heat transfer occurs between the compound drop and its surrounding fluid. The heat transfer characteristics of a partially engulfed gas–liquid compound drop translating in a different immiscible fluid appear to have been first studied by Sideman & Taitel (1964), who used pentane and butane drops as the dispersed phase evaporating in a continuous phase of distilled water. Vuong & Sadhal (1989*b*) computed the evaporation of a pentane drop in glycerol. Dammel & Beer (2003) have studied the case of heat transfer from a continuous liquid to a drop of a second immiscible liquid, which rises due to buoyancy and simultaneously evaporates. In all these studies, the velocity was computed independently from the temperature field. It is known, however, that heat transfer processes can significantly influence the dynamics of interactions of drops and bubbles in non-isothermal multiphase systems. When a bubble or drop is placed in a fluid in which the temperature changes from one place to another, temperature variations are expected at the interface of the fluid particle. The consequence is a variation of the local tension on the surface which causes a tangential surface traction from lower to higher tension regions, which results in motion on both sides of the interface and a net migration of the drop or the bubble normally towards the heat source. We refer to this motion as a thermocapillary or Marangoni migration. The thermocapillary or Marangoni flow is especially important in cases when the natural buoyancy-driven motion is suppressed, e.g. in the absence of gravity force or when the densities of the phases are nearly equal and in microscale systems. Many studies devoted to the thermocapillary migration and interaction of separate drops were aimed to simulate these special applications. A comprehensive review is given in a monograph by Subramanian & Balasubramaniam (2001).

Non-uniformity of a temperature field in a suspension of drops may be imposed not only by a distant boundary condition but it may be caused by heat transfer between phases which eventually results in spontaneous thermocapillary migration by nearby particles towards or apart from each other. Spontaneous thermocapillary effect is typical for several drops, which are not in thermodynamic equilibrium between them or with the ambient phase. The heat transfer that occurs between the phases in

such systems induces non-homogeneous temperature field that causes surface tension gradients and, hence, thermocapillary migration of the dispersed species. The model of spontaneous motion of two separate drops induced by an interfacial mass transfer was first suggested by Golovin, Nir & Pismen (1995) and has been studied subsequently in a series of works by Lavrenteva, Leshansky & Nir (1999), Lavrenteva & Nir (2001), Berejnov *et al.* (2002), Lavrenteva *et al.* (2002) and Bialik-Rosenfeld, Lavrenteva & Nir (2007).

A number of works concerning thermocapillary migration of compound drops with complete engulfment is available in the literature as well. The dynamics of concentric compound drops under externally imposed temperature or surfactant concentration gradient was studied by Stone & Leal (1990), Borhan, Haj-Hariri & Nadim (1992) and Haj-Hariri, Nadim & Borhan (1993). The case of eccentric compound drops was investigated by Morton, Subramanian & Balasubramaniam (1990). The motion that results from both temperature field and residual contaminations applied at the surface of a liquid system was analysed by Lyell & Carpenter (1993). The spontaneous Marangoni migration of a compound drop due to the secretion of a surface-active substance by a completely engulfed droplet at an off-centre location was studied by Tsemakh, Lavrenteva & Nir (2004).

Experimental studies regarding the heat transfer characteristics of a partially engulfed gas–liquid compound drop translating in a different immiscible fluid appear to have been first introduced by Sideman & Taitel (1964). They used pentane and butane drops as the dispersed phase evaporating in a continuous phase of distilled water. Later on, Tochitani *et al.* (1977*a*, *b*) used a highly viscous fluid (glycerol) as the continuous phase, so they were able to maintain the pentane drop close to a spherical shape and the drop rose in a rectilinear manner from the initial to the final states. A simple method to form liquid–gas compound drops is to let air bubbles rise from one liquid into another one above it. The motion of an air bubble rising through a liquid and crossing a plane interface into another immiscible liquid of lower density has been experimentally studied by Mercier *et al.* (1974), Mori *et al.* (1977), Mori (1978) and Hashimoto & Kawano (1990). With distilled water as the lower layer and lighter oil as the upper, it was found by Mercier *et al.* (1974) that the water attaches onto the bubble as it passes upward into the oil. Various mineral oils were used for the upper phase and the observations showed, as would be expected, that with increasing the viscosity of the oil phase, the bubble motion slowed down. In other experiments, Hashimoto & Kawano (1990) observed that configurations more complex than completely engulfed and partially engulfed compound drops come into existence.

The subject of thermocapillary-induced motion of a partially engulfed compound drop remains almost unexplored so far, though most of the processes involving compound drops mentioned above are accompanied by intensive heat transfer and thus a significant influence of the Marangoni effect on these processes may be expected. In our previous work (Rosenfeld, Lavernteva & Nir 2008) we have studied the dynamics of an axisymmetric hybrid drop in an infinite viscous domain. This is the first study of the motion of the partially engulfed compound drop induced by the Marangoni effect due to an imposed linear temperature field. The particular case studied there was limited by the assumption of equal thermal conductivities of all three phases and hence in that case the temperature field remains unperturbed. It was found that, typically, the motion was induced in the direction of the temperature gradient. Nevertheless, some interesting limiting cases in which the hybrid drop moved against the temperature gradient were observed as well.

The aim of the present work is to provide a general study in which the hybrid drop is affected by a temperature field imposed externally or temperature variations caused by spontaneous heat transfer between the phases. In this study we explore the effect of varying physical properties such as thermal conductivities, viscosities and the dependence of surface tension on temperature, as well as the relative volumes of the phases in the compound drop. The important effect of the contact angles at the three-phase boundary is also explored. The results, which are of general nature, are demonstrated via a sequence of particular examples in which the solution of the complex problem is considerably simplified. We begin by studying the thermocapillary motion of a non-conductive and partially conductive compound drops. We further investigate the influence of the conductivity ratio on the motion of the hybrid drop in the case of a compound drop comprised of a spherical drop and an attached spherical segment. We conclude by investigating the spontaneous thermocapillary motion of the partially engulfed compound drop. In § 2 we define the general problem and the differences between the cases of externally imposed temperature field and spontaneous induced temperature variations. The method of solution is described in § 3. In § 4 we describe the details of the various cases examined while in § 5 we depict and discuss the calculated results.

2. Statement of the problem

Consider a partially engulfed compound fluid drop in which the phases are immiscible, which is embedded in a non-isothermal viscous medium. A schematic description of the drop is depicted in figure 1.

The compound drop consists of two phases and posses three fluid–fluid interfaces that intersect at a three-fluid contact line. We assume that the surface forces dominate over the viscous forces and that the interfaces do not deform due to the motion and preserve their static configuration. Following Torza & Mason (1970) we conclude that, in the absence of an external body force, the interfaces are spherical segments intersecting at contact angles, which are determined by the force balance at the triple junction, $\cos\theta_i = (\gamma_{jk}^2 - \gamma_{ij}^2 - \gamma_{ik}^2)/(2\gamma_{ij}\gamma_{ik})$, with i, j and k denoting the various phases (no summation), and γ_{ij} $(i \neq j \neq k = 1, 2, 3)$ being the interfacial tensions. The final equilibrium configuration of the compound drop is determined by these angles and by the volume ratio in the hybrid body.

2.1. *The hydrodynamic problem*

When inertia forces are negligible the governing equations for the above system are the linearized Stokes equations, and have the following form:

$$\nabla \cdot \boldsymbol{u} = 0 \tag{2.1}$$

$$\nabla \cdot \boldsymbol{\sigma} = 0, \quad \boldsymbol{\sigma} = -p\boldsymbol{I} + \mu_i(\nabla \boldsymbol{u} + \nabla \boldsymbol{u}^T), \tag{2.2}$$

where $i = 1, 2, 3$, is used to denote dispersed and continuous liquid phases, respectively (see figure 1). $\boldsymbol{u}$, p and σ are the velocity, pressure and stress fields in the respective domain, while μ_i denotes the viscosity in phase i. The boundaries between phases i and j are denoted by Γ_{ij}. For a drop moving with a constant velocity $U \cdot \boldsymbol{i}_z$ in an otherwise quiescent fluid, we consider a problem in a reference frame linked to the drop for which the boundary and interfacial conditions are

$$\boldsymbol{u} = -U \cdot \boldsymbol{i}_z @ \ |\boldsymbol{r}| \to \infty, \tag{2.3}$$

where $\boldsymbol{i}_z$ is a unit vector in the z-direction (see figure1),

$$[\boldsymbol{u}] = 0, \quad \boldsymbol{r} \in \Gamma_{ij}, \quad i = 1, 2;\ j = 2, 3;\ i \neq j. \tag{2.4}$$

Since the motion and geometry are steady,

$$\boldsymbol{u} \cdot \boldsymbol{n} = 0, \quad \boldsymbol{r} \in \Gamma_{ij}, \quad i = 1, 2;\ j = 2, 3;\ i \neq j. \tag{2.5}$$

For interfaces having spherical segment shapes the normal stress differences are satisfied at the leading order of vanishingly small capillary number by a uniform stress jump.

The tangential stress balance obtains the form

$$\boldsymbol{n} \cdot [\boldsymbol{\sigma}] \cdot \boldsymbol{\tau} = -\frac{\partial \gamma}{\partial \tau}, \quad \boldsymbol{r} \in \Gamma_{ij}, \quad i = 1, 2;\ j = 2, 3;\ i \neq j. \tag{2.6}$$

In (2.3)–(2.6), $\boldsymbol{n}$ is a unit vector normal to the surface (see figure 1), [ ] denotes the jump across each surface of the drop from the outside to the inside and $\boldsymbol{\tau}$ is a unit vector tangent to the surface.

The interfacial tension γ is, in general, a function of the thermodynamic state variables. In this work, we assume that $\gamma = \gamma(T)$, where T is the local temperature. We shall consider, henceforth, various cases of non-isothermal environments in which the temperature variation along the interfaces is induced either by externally imposed fields or by transport of heat between the phases due to deviation from thermodynamic equilibrium.

2.2. *The thermal problem*

In the case of an externally imposed temperature field, we assume that the continuous phase (phase 2) experiences a constant temperature gradient at infinity $\nabla T(|\boldsymbol{r}| \to \infty) = \nabla T_\infty \boldsymbol{i}_z$, with $\nabla T_\infty = const$. This imposed temperature field results in local temperature variations in the vicinity of the hybrid drop at the interfaces Γ_{12}, Γ_{13} and Γ_{23}, and hence a variation of the local tension on the surface is induced. The latter causes a tangential surface traction from lower tension regions towards regions with higher interfacial tension and a net motion of the entire compound drop.

For the temperature field we need to calculate the heat transfer balance around and inside the compound drop. It is assumed that the respective Péclet numbers of the three phases are vanishingly small, which means that heat conduction is the governing transport mechanism while convective effect is negligible. Hence, the heat balance is reduced to the Laplace equation

$$\nabla^2 T = 0. \tag{2.7}$$

The boundary conditions are as follows:

$$T \to \nabla T_\infty z @ |\boldsymbol{r}| \to \infty, \tag{2.8}$$

$$[T] = 0, \quad \boldsymbol{r} \in \Gamma_{ij}; \quad i = 1, 2;\ j = 2, 3;\ i \neq j, \tag{2.9}$$

$$[\boldsymbol{q} \cdot \boldsymbol{n}] = 0, \quad \boldsymbol{r} \in \Gamma_{ij}; \quad i = 1, 2;\ j = 2, 3;\ i \neq j, \tag{2.10}$$

where $\boldsymbol{q} = -\kappa_i \nabla T$, with κ_i being the thermal conductivity, is the heat flux.

Non-uniformity of a temperature field in a suspension of drops may be imposed by distant boundary condition (as in the previous case) or it may be caused by heat transfer between the phases that eventually results in a spontaneous thermocapillary migration of the fluid particles. For example, consider a case of spontaneous thermocapillary motion where phase 1 has initially a constant temperature T_S different from that of phases 2 and 3, T_0. Assume also that $\kappa_1 \to \infty$, and thus the interfaces

Γ_{12} and Γ_{13} are of uniform temperature T_S. The heat conducts from these surfaces towards Γ_{23} and hence causes temperature distribution on the latter which induces the motion of the entire compound drop due to the Marangoni effect.

The heat transfer problem in this case is similar to the case of an external temperature gradient (2.7) but with the following conditions:

$$T_2 = T_S \ @ \ \boldsymbol{r} \in \Gamma_{12}, \quad T_3 = T_S \ @ \ \boldsymbol{r} \in \Gamma_{13}, \tag{2.11}$$

$$T_2 \to T_0 \ @ \ |\boldsymbol{r}| \to \infty. \tag{2.12}$$

And conditions (2.9) and (2.10) are satisfied on Γ_{23}.

The solution of the problems defined above produce the temperature fields, which in turn affect the variation of the surface tension on the various interfaces via condition (2.6).

3. Method of solution, flow field

We render the length, velocity, stream function and stress non-dimensional using R, U_M, R^2U_M and $\mu_2 U_M/R$, respectively, where U_M denotes a reference velocity to be defined and R is defined as the radius of a sphere having the same volume as the total compound drop, i.e. $4/3\pi R^3 = V_1 + V_3$.

The problem formulated above is axisymmetric. Instead of solving for the velocity and pressure distributions we choose to use Stokes stream function ψ.

The general solution for the stream function can be written as in Payne & Pell (1960) and Vuong & Sadhal (1989*a*) (see also the Appendix for more details)

$$\psi^{(i)}(\xi, \eta) = \frac{1}{(\cosh\xi - \cos\eta)^{3/2}} \int_0^\infty \phi^{(i)}(\eta, \lambda) \sinh^2\xi \, P'_{-1/2+i\lambda}(\cosh\xi)\, \mathrm{d}\lambda \quad i = 1, 2, 3, \tag{3.1}$$

where $P'_{-1/2+i\lambda}$ is the derivative of the Legendre function with respect to its argument and $\phi(\eta, \lambda)$ consists of a combination of four linearly independent expressions

$$\phi^{(i)}(\lambda, \eta) = \cos\eta[A^{(i)}(\lambda)\cosh\lambda\eta + B^{(i)}(\lambda)\sinh\lambda\eta] + \sin\eta[C^{(i)}(\lambda)\cosh\lambda\eta + D^{(i)}(\lambda)\sinh\lambda\eta]. \tag{3.2}$$

When the distribution of temperature along the interfaces, which determines the right-hand side of (2.6), is known, the coefficients $A^{(i)}(\lambda)$, $B^{(i)}(\lambda)$, $C^{(i)}(\lambda)$ and $D^{(i)}(\lambda)$ are determined using the boundary conditions (2.3)–(2.6). The procedure of finding these coefficients was developed by Rosenfeld *et al.* (2008) following methods of Oğuz (1987) and Vuong and Sadhal (1989*a*), who solved the problem of the compound drop motion in the absence of Marangoni effect. The details of methods of calculation are given in the Appendix.

In this analysis we follow a procedure common to previous analyses of thermo-capillary-induced dynamics. We assume that the temperature variation changes the interfacial tensions, but we neglect the effect on all other bulk and surface physical properties. This assumption follows the Boussinesq approximation, that is also applied in analyses of free convection, where only the property that drives the motion is perturbed. It is meant to emphasize this primary effect and isolate it from all other secondary effects. The interfacial tension is considered to depend linearly on the temperature. Indeed, for large temperature variations it is not expected to be linear as otherwise negative tensions may arise, however, capillary and thermcapillary effects

are particularly significant for drops and bubbles of small size, at which scale this dependence can be well approximated to be linear with a good accuracy. We assume, thus, that the surface tension has the form $\gamma = 1 + \gamma_T(T/T_0 - 1)$, where T_0 denotes the temperature at the origin ($\rho = z = 0$) for the case of external gradient field or the constant temperature far from the drop for the case of spontaneous Marangoni motion. γ is normalized by the value of the tension $\hat{\gamma}(T_0)$ at the inner interface Γ_{13} and γ_T denotes $\partial\gamma/\partial T$ at each interface, a constant value which in most cases is negative. Also the Marangoni velocity, in which all velocities are scaled, is being defined as $U_M = R\overline{\nabla T}|\gamma_T^{13}|/\mu_2$, where $\overline{\nabla T} = \nabla T_\infty$ for the case of externally imposed temperature field while $\overline{\nabla T} = (T_S - T_0)/R$ for the spontaneous thermocapillary-induced motion. These assumptions are conventional in the theory of Marangoni migration of drops and bubbles (see e.g. Subramanian & Balasubramaniam 2001, for additional discussion).

We further assume that, since the typical capillary number $Ca = \mu_2 U/\hat{\gamma}$ is vanishingly small, although the surface tension varies along the interfaces, its variation is not strong enough to cause non-negligible changes in the contact angles and the configuration of the drop during its motion.

The temperature field is coupled with the flow field via the stress boundary condition. The tangential stress condition (2.6) in terms of the stream function is of the form

$$\frac{(\cosh\xi - \cos\eta_{ij})^{3/2}}{c^2 \sinh\xi} \int_0^\infty \left(\frac{\partial^2 \phi^{(i)}}{\partial \eta^2} - \frac{\mu_j}{\mu_i} \frac{\partial^2 \phi^{(j)}}{\partial \eta^2} \right) \sinh^2\xi \, P'_{-1/2+i\lambda}(\cosh\xi) \mathrm{d}\lambda = \pm h \frac{\partial T_{ij}}{\partial \xi}, \tag{3.3}$$

where the (+) sign applies at Γ_{12} and Γ_{13} and the (−) sign at Γ_{23}. T_{ij} denotes the temperature on Γ_{ij} and $h = (\cosh\xi - \cos\eta)/c$ is a metric coefficient.

The viscous drag force due to the disturbance velocity on the compound drop is calculated using the asymptotic expression given by Payne & Pell (1960)

$$\frac{F}{8\pi\mu_2 R U_M} = \lim_{r\to\infty} \frac{\rho\psi^{(2)}}{r^2}, \tag{3.4}$$

where $r = \sqrt{\rho^2 + z^2}$ and $\psi^{(2)}$ is the disturbance stream function in the ambient fluid which decays at $r \to \infty$. This expression reduces to

$$\frac{F}{8\pi\mu_2 R U_M} = \frac{1}{2} + \frac{1}{\sqrt{2}} \int_0^\infty \left(\phi^{(2)}_{total}(0,\lambda) - UN(0,\lambda) \right) \left(\lambda^2 + \frac{1}{4} \right) \mathrm{d}\lambda, \tag{3.5}$$

where the equality $P'_{-1/2+i\lambda}(1) = -1/2(\lambda^2 + 1/4)$ was applied.

The requirement that the total viscous force on the drop vanishes provides the velocity of the drops' migration in the temperature field U.

4. Temperature field

In this section, we consider various cases involving particular temperature fields. The temperature is scaled by $R\,\nabla T_\infty$ for the cases involving external gradient, and by $T_S - T_0$ for the spontaneous Marangoni motion.

4.1. *Non-conducting compound drop in an external temperature gradient*

In this case, it is assumed that the compound drop has low conductivity and hence the stress variations occur at the outer interfaces Γ_{12} and Γ_{23}. In order to find the temperature field around the compound drop we have used the approach presented by

Sadhal (1983) and extended by Feuillebois (1989) and Loewenberg & Davis (1993*a*, *b*). The idea is to calculate directly the heat flux in the form

$$\boldsymbol{q} = \nabla \times \left(\frac{\Phi}{\rho} \boldsymbol{i}_\phi \right), \tag{4.1}$$

where Φ is an unknown function. Calculating the curl in cylindrical coordinates, expression (4.1) is written explicitly

$$\boldsymbol{q} = -\boldsymbol{i}_\rho \frac{1}{\rho} \frac{\partial \Phi}{\partial z} + \boldsymbol{i}_z \frac{1}{\rho} \frac{\partial \Phi}{\partial \rho}. \tag{4.2}$$

The flux $\boldsymbol{q}$ may also be represented as a gradient of a potential T by the Fourier law, $\boldsymbol{q} = -\kappa \nabla T$, where κ is the thermal conductivity. Therefore, we can conclude that $\nabla \times \boldsymbol{q} = -\kappa \nabla \times \nabla T = 0$ which leads to

$$L_{-1}(\Phi) = 0, \tag{4.3}$$

where L_{-1} is the axisymmetric Stokes operator (see the Appendix). Using the toroidal coordinate system, the components of the heat flux are

$$q_\xi = \frac{(\cosh \xi - \cos \eta)^2}{c^2 \sinh \xi} \frac{\partial \Phi}{\partial \eta}, \tag{4.4}$$

$$q_\eta = -\frac{(\cosh \xi - \cos \eta)^2}{c^2 \sinh \xi} \frac{\partial \Phi}{\partial \xi}. \tag{4.5}$$

The appropriate boundary conditions (2.8)–(2.10) take the form

$$\Phi_2|_{\xi,\eta \to 0} = -\frac{\kappa_2 \rho^2}{2} = -\frac{\kappa_2}{2} \left(\frac{\sinh \xi}{\cosh \xi - \cos \eta} \right)^2 \text{ at infinity} \tag{4.6}$$

while

$$\left. \frac{\partial \Phi_2}{\partial \xi} \right|_{\eta_{12}, \eta_{23}} = 0. \tag{4.7}$$

It follows from (4.7) that at the interfaces $\Phi_2|_{\eta_{12}, \eta_{23}}$ is constant which, without loss of generality, is chosen to be zero.

The general solution for (4.3) satisfying (4.6) may be written in the form

$$\Phi_2 = (\cosh \xi - \cos \eta)^{-1/2} \int_0^\infty \left(\beta_2(\lambda, \eta) + \frac{\kappa_2 \sqrt{2} \cosh(\lambda(\pi - \eta))}{\cosh \lambda \pi} \right) \sinh^2 \xi \, P'_{-1/2+i\lambda} \times (\cosh \xi) \, \mathrm{d}\lambda, \tag{4.8}$$

where, $\beta_2 = B_1(\lambda) \cosh(\lambda \eta) + B_2(\lambda) \sinh(\lambda \eta)$. $B_1(\lambda)$ and $B_2(\lambda)$ are to be determined using the boundary conditions (4.7).

$$B_1 = \frac{\sqrt{2} \kappa_2 \, (\cosh((\pi - \eta_{12})\lambda) \sinh(\eta_{23}\lambda) - \cosh((\pi + \eta_{23})\lambda) \sinh(\eta_{12}\lambda))}{\sinh((\eta_{12} - \eta_{23})\lambda) \cosh(\lambda \pi)}, \tag{4.9}$$

$$B_2 = \frac{\sqrt{2} \kappa_2 \, \sinh((\eta_{12} + \eta_{23})\lambda) \tanh(\lambda \pi)}{\sinh((\eta_{12} - \eta_{23})\lambda)}. \tag{4.10}$$

The right-hand side of the stress boundary condition (3.3) can be written as

$$h \left. \frac{\partial T_2}{\partial \xi} \right|_{\eta_{12}, \eta_{23}} = -\left. \frac{q_{2\xi}}{\kappa_2} \right|_{\eta_{12}, \eta_{23}} = -\frac{(\cosh \xi - \cos \eta)^2}{c^2 \sinh \xi} \left. \frac{\partial \Phi_2}{\partial \eta} \right|_{\eta_{12}, \eta_{23}} \tag{4.11}$$

and the stress boundary condition becomes

$$\left(\frac{\partial^2\phi^{(2)}}{\partial\eta^2}-\frac{\mu_1}{\mu_2}\frac{\partial^2\phi^{(1)}}{\partial\eta^2}\right)\Bigg|_{\eta_{12}}=-\left(\frac{\partial\beta_2}{\partial\eta}\Bigg|_{\eta_{12}}-\frac{\kappa_2\sqrt{2}\lambda\sinh\left(\lambda\left(\pi-\eta_{12}\right)\right)}{\cosh\lambda\pi}\right), \tag{4.12}$$

$$\left(\frac{\partial^2\phi^{(2)}}{\partial\eta^2}-\frac{\mu_3}{\mu_2}\frac{\partial^2\phi^{(3)}}{\partial\eta^2}\right)\Bigg|_{\eta_{23}}=\frac{\partial\beta_2}{\partial\eta}\Bigg|_{\eta_{23}}+\frac{\kappa_2\sqrt{2}\lambda\sinh\left(\lambda\left(\pi+\eta_{23}\right)\right)}{\cosh\lambda\pi}. \tag{4.13}$$

4.2. *Partially conducting compound drop, $\kappa_1=0$, $\kappa_2=\kappa_3$, in an external temperature gradient*

In this case, we have assumed that the phase 1 is non-conductive and the conductivities of phases 2 and 3 are equal. The method of solution is similar to that of the case of non-conducting compound drop described above. The boundary conditions are

$$\Phi_2|_{\eta_{12}}=\Phi_3|_{\eta_{13}}=0, \tag{4.14}$$

$$\Phi_2|_{\eta_{23}}=\Phi_3|_{\eta_{23}}, \tag{4.15}$$

$$\frac{\partial\Phi_2}{\partial\eta}\Bigg|_{\eta_{23}}=\frac{\partial\Phi_3}{\partial\eta}\Bigg|_{\eta_{23}}, \tag{4.16}$$

where $\Phi_3=(\cosh\xi-\cos\eta)^{-1/2}\int_0^\infty\beta_3(\lambda,\eta)\sinh^2\xi\,P'_{-1/2+i\lambda}(\cosh\xi)\mathrm{d}\lambda$ with $\beta_3=B_3(\lambda)\cosh(\lambda\eta)+B_4(\lambda)\sinh(\lambda\eta)$ and Φ_2 as in (4.8).

The tangential heat flux at the 2–3 interface is

$$q_\xi\Big|_{\eta_{23}}=\frac{(\cosh\xi-\cos\eta_{23})^2}{c^2\sinh\xi}\frac{\partial\Phi_3}{\partial\eta}\Bigg|_{\eta_{23}}=\frac{(\cosh\xi-\cos\eta_{23})^{1/2}\sinh\xi}{c^2}\times\int_0^\infty\left[(\cosh\xi-\cos\eta_{23})\frac{\partial\beta_3}{\partial\eta}\Bigg|_{\eta_{23}}-\sin\eta_{23}\beta_3(\lambda,\eta_{23})\right]P'_{-1/2+i\lambda}(\cosh\xi)\,\mathrm{d}\lambda \tag{4.17}$$

and the stress boundary condition takes the form

$$\int_0^\infty\frac{\partial^2\phi^{(2)}}{\partial\eta^2}-\frac{\mu_3}{\mu_2}\frac{\partial^2\phi^{(3)}}{\partial\eta^2}\Bigg|_{\eta_{23}}P'_{-1/2+i\lambda}(\cosh\xi)\,\mathrm{d}\lambda=-\frac{1}{\kappa_3(\cosh\xi-\cos\eta_{23})}\times\int_0^\infty\left[(\cosh\xi-\cos\eta_{23})\frac{\partial\beta_3}{\partial\eta}\Bigg|_{\eta_{23}}-\sin\eta_{23}\beta_3(\lambda,\eta_{23})\right]P'_{-1/2+i\lambda}(\cosh\xi)\,\mathrm{d}\lambda. \tag{4.18}$$

Using the Mehler–Fock transform of order one given by Sneddon (1972) and Zabarankin (2007),

$$\left.\begin{aligned}H(\xi)&=-\int_0^\infty\lambda\tanh(\lambda\pi)\hat{H}(\lambda)P'_{-1/2+i\lambda}(\cosh\xi)d\lambda\\\hat{H}(\lambda)&=\int_0^\infty\frac{H(\xi)\sinh\xi\,P'_{-1/2+i\lambda}(\cosh\xi)}{(\lambda^2-1/4)}\,\mathrm{d}\xi\end{aligned}\right\} \tag{4.19}$$

on the right-hand side of (4.18) yields for the stress boundary condition at Γ_{23}

$$\frac{\partial^2\phi^{(2)}}{\partial\eta^2}-\frac{\mu_3}{\mu_2}\frac{\partial\phi^{(3)}}{\partial\eta^2}\Bigg|_{\eta_{23}}=-\frac{\lambda\tanh(\lambda\pi)}{(\lambda^2-1/4)}\int_0^\infty H_1(\xi)\sinh\xi\,P'_{-1/2+i\lambda}(\cosh\xi)\,\mathrm{d}\xi, \tag{4.20}$$

where

$$H_1(\xi)=-\frac{1}{\kappa_3(\cosh\xi-\cos\eta_{23})}\int_0^\infty\left[(\cosh\xi-\cos\eta_{23})\frac{\partial\beta_3}{\partial\eta}\Bigg|_{\eta_{23}}-\sin\eta_{23}\beta_3(\lambda,\eta_{23})\right]\times P'_{-1/2+i\lambda}(\cosh\xi)\,\mathrm{d}\lambda.$$

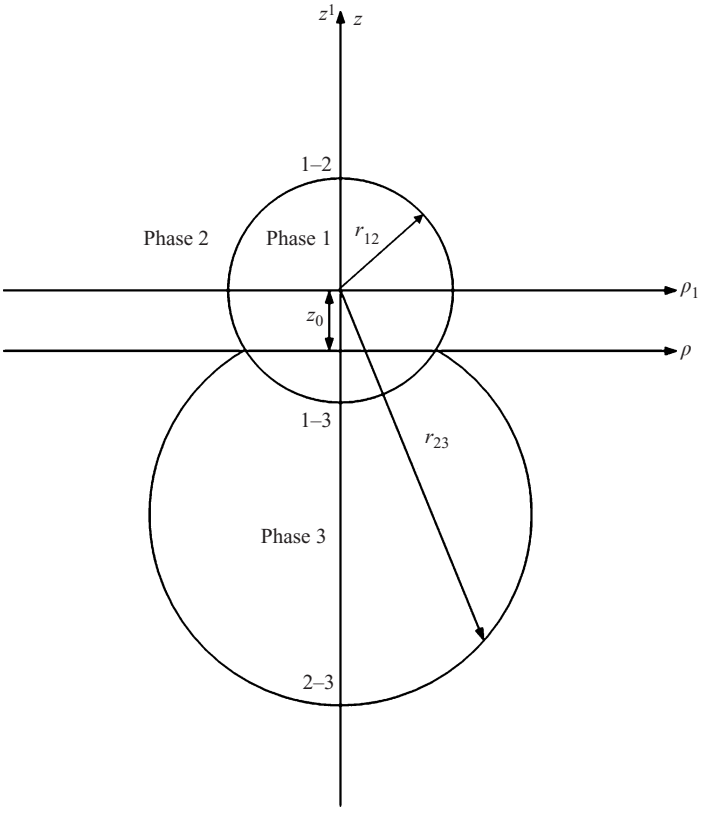

FIGURE 2. Schematic descriptions of a compound drop in which phase 1 is a complete sphere.

4.3. *Compound drop in which phase 1 is a complete sphere, in an external temperature gradient*

A schematic description of this assembly is presented in figure 2.

Here, ρ', z' are the cylindrical coordinates connected to the spherical system centred in phase 1 and ρ, z are the cylindrical coordinates attached to the toroidal system. The two cylindrical systems are related through $\rho = \rho'$; $z = z' - z_0$; $r = (\rho'^2 + z'^2)^{1/2} = (\rho^2 + (z - z_0)^2)^{1/2}$.

The temperature distribution for this drop when embedded in an external field is found by solving the temperature problem in spherical coordinates centred in phase 1. Applying the appropriate boundary conditions (continuity of the heat flux at the interfaces), we found that, in the case of equal heat conductivities of phases 2 and 3, $\kappa_2 = \kappa_3$, the temperature fields are

$$T_1 = \frac{3\kappa_2}{\kappa_1 + 2\kappa_2} r \cos\theta, \tag{4.21}$$

$$T_{2,3} = \left[r + \left(\frac{\kappa_2 - \kappa_1}{\kappa_1 + 2\kappa_2} \right) r^{-2} \right] \cos\theta. \tag{4.22}$$

The temperature fields in terms of toroidal coordinates obtain the form

$$T_1 = \frac{3\kappa_2}{\kappa_1 + 2\kappa_2}\left[\frac{c\sin\eta}{(\cosh\xi - \cos\eta)} + z_0\right], \tag{4.23}$$

$$T_{2,3} = \left(z_0 + \frac{c\sin\eta}{(\cosh\xi - \cos\eta)}\right) \times \left[1 + \frac{(\kappa_2 - \kappa_1)/(\kappa_1 + 2\kappa_2)}{((z_0 + c\sin\eta/(\cosh\xi - \cos\eta))^2 + c^2\sinh^2\xi/(\cosh\xi - \cos\eta)^2)^{3/2}}\right] \tag{4.24}$$

where, $z_0 = c\cot\eta_{12}$. The tangential stress boundary conditions become

$$\frac{\partial^2\phi^{(2)}}{\partial\eta^2} - \frac{\mu_1}{\mu_2}\frac{\partial^2\phi^{(3)}}{\partial\eta^2}\bigg|_{\eta_{12}} = \frac{3\kappa_2}{\kappa_1 + 2\kappa_2}\frac{4\sqrt{2}}{3}\frac{\lambda\sinh(\lambda(\pi - \eta_{12}))}{\cosh\lambda\pi}, \tag{4.25}$$

$$\frac{\partial^2\phi^{(3)}}{\partial\eta^2} - \frac{\mu_1}{\mu_3}\frac{\partial^2\phi^{(1)}}{\partial\eta^2}\bigg|_{\eta_{13}} = \frac{3\kappa_2}{\kappa_1 + 2\kappa_2}\frac{4\sqrt{2}}{3}\frac{\lambda\sinh(\lambda(\pi + \eta_{13}))}{\cosh\lambda\pi} \tag{4.26}$$

and

$$\frac{\partial^2\phi^{(2)}}{\partial\eta^2} - \frac{\mu_3}{\mu_2}\frac{\partial^2\phi^{(3)}}{\partial\eta^2}\bigg|_{\eta_{23}} = -\frac{\lambda\tanh(\lambda\pi)}{(\lambda^2 - 1/4)} \times \int_0^\infty \frac{c}{(\cosh\xi - \cos\eta_{23})^{1/2}}\frac{\partial T_2}{\partial\xi}\sinh\xi\, P'_{-1/2+i\lambda}(\cosh\xi)\,\mathrm{d}\xi. \tag{4.27}$$

4.4. *Spontaneous thermocapillary motion*

Here, we have assumed that the interfaces Γ_{12} and Γ_{13} are of uniform temperature T_S and that $\kappa_2 = \kappa_3$. The tangential temperature gradient is induced on Γ_{23} by the heat that is conducting from Γ_{12} and Γ_{13} towards that surface, thereby inducing a non-uniform temperature distribution on it. The temperature in phases 2 and 3 is found in toroidal coordinates to be (Lebedev 1965)

$$T = \frac{T_0}{T_S - T_0} + (\cosh\xi - \cos\eta)^{1/2}\int_0^\infty G(\eta, \lambda)P_{-1/2+i\lambda}(\cosh\xi)\,\mathrm{d}\lambda, \tag{4.28}$$

where $G = C_1(\lambda)\cosh\lambda\eta + C_2(\lambda)\sinh\lambda\eta$. $C_1(\lambda)$ and $C_2(\lambda)$ are to be determined using the boundary conditions $T_2|_{\eta_{12}} = T_2|_{\eta_{13}} = T_S$.

$$C_1 = \frac{\sqrt{2}\,(\cosh((\pi + \eta_{13})\,\lambda)\sinh(\eta_{12}\lambda) - \cosh((\pi - \eta_{12})\,\lambda)\sinh(\eta_{13}\lambda))}{\sinh((\eta_{12} - \eta_{13})\,\lambda)\cosh(\lambda\pi)}, \tag{4.29}$$

$$C_2 = \frac{\sqrt{2}\,(\cosh((\pi - \eta_{12})\,\lambda)\cosh(\eta_{13}\lambda) - \cosh(\eta_{12}\lambda)\cosh((\pi + \eta_{13})\,\lambda))}{\sinh((\eta_{12} - \eta_{13})\,\lambda)\cosh(\lambda\pi)}. \tag{4.30}$$

The stress boundary condition at the interface Γ_{23} takes the form

$$\frac{\partial^2\phi^{(2)}}{\partial\eta^2} - \frac{\mu_3}{\mu_2}\frac{\partial^2\phi^{(3)}}{\partial\eta^2} = -\frac{\lambda\tanh\lambda\pi}{(\lambda^2 - 1/4)}\int_0^\infty g(\xi)\sinh\xi\, P'_{-1/2+i\lambda}(\cosh\xi)\,\mathrm{d}\xi \tag{4.31}$$

with,

$$g(\xi) = \frac{c}{2(\cosh\xi - \cos\eta_{23})} \int_0^\infty G(\eta_{23}, \lambda)[P_{-1/2+i\lambda}(\cosh\xi) + 2(\cosh\xi - \cos\eta)P'_{-1/2+i\lambda}(\cosh\xi)]\mathrm{d}\lambda.$$

5. Results and discussion

5.1. *The case of a non-conducting compound drop moving under the influence of an external temperature gradient*

When the thermocapillary-induced motion is the outcome of an imposed constant distant external temperature gradient, the ambient fluid and the compound drop are not isothermal and hence local temperature gradients appear along the interfaces. This results in tangential stresses that, in turn, induce motion of the interfaces and the adjacent fluids. Here we have assumed that the two dispersed phases comprising the compound drop are non-conductive and hence the thermally active interfaces are the outer ones Γ_{12}, Γ_{23}. Here and below, an interface at which Marangoni effect takes place (the right-hand side of the tangential stress balance is non-zero) is referred to as 'thermally active'. While an interface is referred to as 'thermally inert' if it is isothermal or its surface tension does not depend on temperature.

Figure 3(a) presents the velocity of the non-conductive compound drop induced by an imposed temperature gradient versus the volume ratio of the two dispersed phases with viscosity ratio μ_1/μ_3 as a parameter ($\mu_2 = \mu_3$). The total volume of the compound drop is kept constant at $4/3\pi$ while the volume ratio is varied. As a first example, the contact angles are determined using specific surface tension values quoted by Vuong & Sadhal (1989a, b), which results in $\theta_1 = 0.8722\pi$, $\theta_2 = 0.95\pi$, $\theta_3 = 0.1778\pi$. Gravity effects were neglected and, for simplicity, we assumed that all derivatives of the three normalized interfacial tensions with respect to the temperature γ_T are equal. The limit $V_1/V_3 \to \infty$ and $\mu_1/\mu_3 \to 0$ simulates a drop that consists mostly of vapour and the velocity approaches the velocity of a non-conductive bubble moving under the influence of an external temperature gradient, as was derived by Young, Goldstein & Block (1959). On the other hand, when $V_1/V_3 \to 0$ the compound drop consists mostly of the fluid phase 3 and hence, for all viscosity ratios, the velocity approaches the value of the velocity of a non-conductive single liquid drop moving under the influence of an external temperature field. Note that, for a very large viscosity ratio $\mu_1/\mu_3 \to \infty$, the change in velocity appears to be monotonic and tends to zero as the volume ratio increases. This case corresponds to phase 1 approaching a solid particle with which we expect no thermocapillary effect. However, when the viscosity ratio diminishes the transition between small and large volume ratios exhibit a minimum in the induced velocity, which is evident around μ_1/μ_3 being of $O(1)$. The velocity versus volume ratio for a different set of contact angles $\theta_1 = 1.02\pi$, $\theta_2 = 0.5\pi$, $\theta_3 = 0.48\pi$ is depicted in figure 3(b). It can be seen that the shape and tendency of the curves is similar to that in the former case (figure 3a), however, the minima evident in figure 3(a) are less pronounced here. Configurations of the compound drops with these sets of contact angles are shown in figure 3 for small, unity and large volume ratios.

5.2. *Partially conducting compound drop in an external temperature gradient*

In this subsection we have considered phase 1 to be non-conductive while the conductivities of the other two phases are equal. Here we have examined two cases.

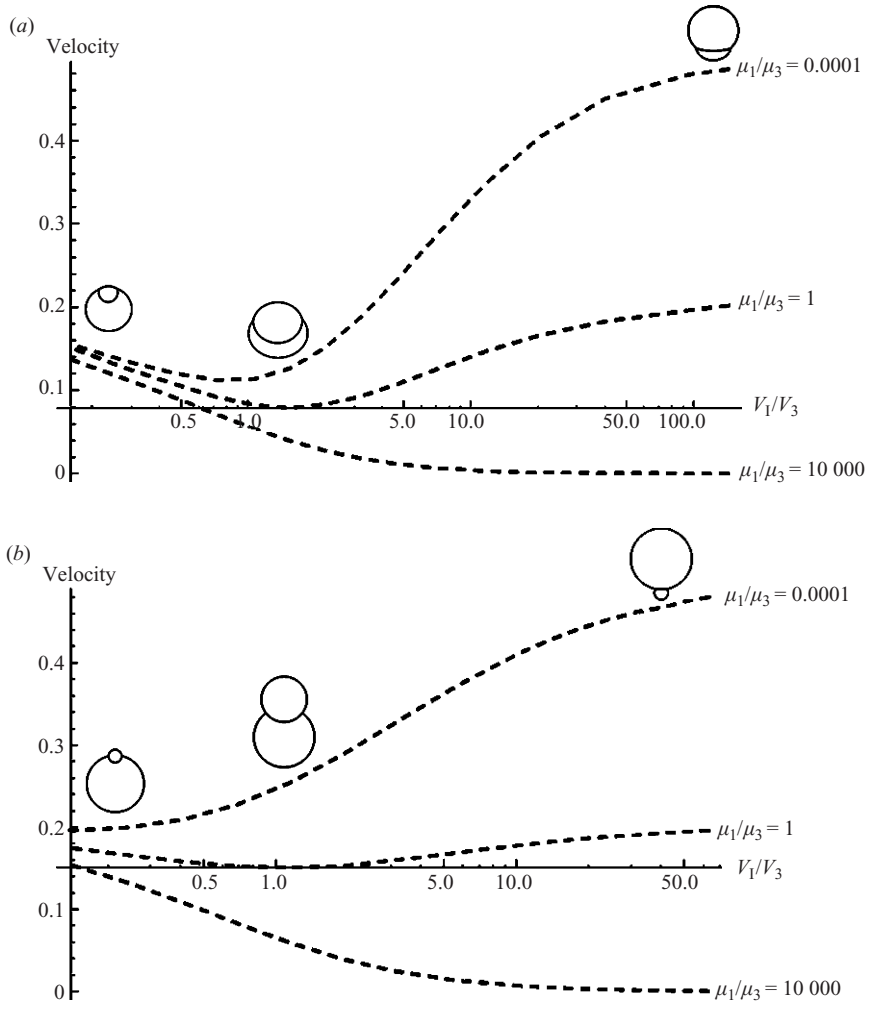

FIGURE 3. Velocity versus volume ratio for various viscosity ratios of the dispersed phases for the case of non-conducting compound drop. $\gamma_T = 1$ on all interfaces; $\kappa_1 = \kappa_3 = 0$, $\kappa_2 = 1$; $\mu_2 = \mu_3 = 1$. The contact angles are (*a*) $\theta_1 = 0.8722\pi$, $\theta_2 = 0.95\pi$, $\theta_3 = 0.1778\pi$; (*b*) $\theta_1 = 1.02\pi$, $\theta_2 = 0.5\pi$, $\theta_3 = 0.48\pi$.

The first one describes the thermocapillary motion of the compound drop due to the external temperature gradient when all the interfaces are thermally active and hence the motion is the outcome of surface tension variations on all the three surfaces. Interesting results emerge from the examination of the case in which the lower interface (Γ_{23}) is thermally inert and its tension does not depend on temperature. Here, the non-uniform temperature distribution and the consequent surface tension gradients take place solely at the interfaces Γ_{12} and Γ_{13}. Results regarding the first case are presented in figure 4. One can see that for $V_1/V_3 \to 0$ the value of the velocity approaches the value of the velocity of a spherical liquid conducting droplet moving under the influence of a distant temperature gradient for all viscosity ratios. On the other hand, when $V_1/V_3 \to \infty$ the velocity varies with the viscosity ratio from the value associated with a bubble moving under the influence of an external temperature

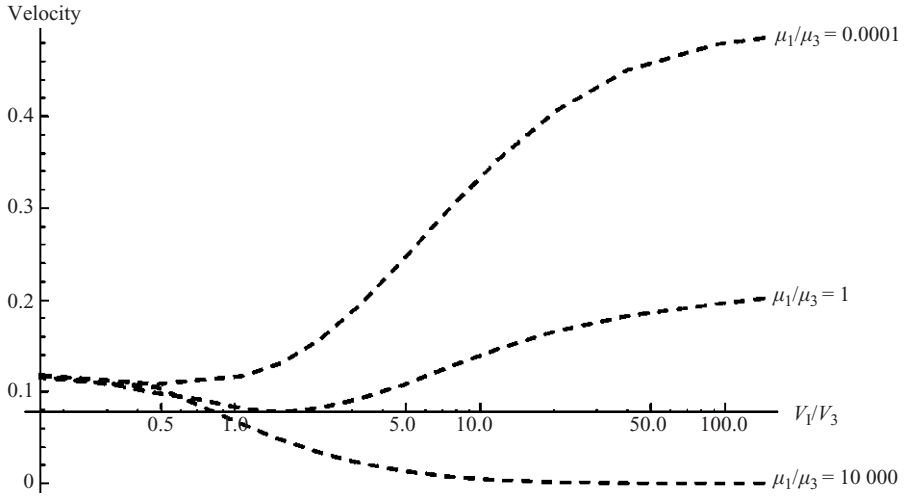

FIGURE 4. Velocity versus volume ratio for various viscosity ratios of the dispersed phases for the case of partially conducting compound drop with all the interfaces thermally active. The contact angles are $\theta_1 = 0.8722\pi$, $\theta_2 = 0.95\pi$, $\theta_3 = 0.1778\pi$; $\gamma_T = 1$ on all interfaces; $\kappa_1 = 0$, $\kappa_3 = \kappa_2 = 1$; $\mu_2 = \mu_3 = 1$.

field through the value typical to a fluid particle with $\mu_1/\mu_3 = O(1)$ and tends to zero for a high viscosity ratio, illustrating a solid particle.

In figure 5(a) the second case in which the lower interface Γ_{23} is thermally inert is depicted. It is interesting to see that when $V_1/V_3 \to 0$ the velocity changes its sign, which indicates that the drop starts to move in the direction opposite to the temperature gradient. This change of the direction of motion of the compound drop occurs since, when the drop is comprised mostly of phase 3 and with the appropriate set of contact angles, the motion of the inner interface Γ_{13} due to surface tension variations is the major driving force for the entire compound drop. Thermocapillary effect results in the flow of liquid near this interface in the direction opposite to the temperature gradient. Since the external boundaries are relatively inert and the motion is induced solely by the Marangoni effect at the internal interface, the flow in their vicinity occurs in the opposite direction (the direction of temperature gradient). As a result, we observe rather the unexpected phenomenon: the drop moving against the temperature gradient (downwards). The same effect takes place if the outer boundaries of a compound drop are thermally active but the internal surface force induces a flow on the external surfaces in the temperature gradient direction. For the cases depicted in figure 5(a), this is the case of relatively small volume ratio, where the inner interface is substantially larger than the upper external one (see sketch of the shape in figure 3a) and the lower one is thermally inert. In contrast to this, when all the interfaces are equally active (the case depicted in figure 4), the effect of the internal interface is always smaller than that of the outer ones and the compound drop migrates to warmer fluid regions as a single-phase drop.

Figure 5(b) presents a similar calculation with a different set of contact angles. It can be seen that in this case the phenomenon of motion against the temperature gradient is not observed even for very small values of the volume ratio (V_1/V_3) since, in this case, the effect of the upper interface is never less important than that at the inner one (see shapes in figure 5b) and, thus, the Marangoni effect at the latter can never overcome the one at the former.

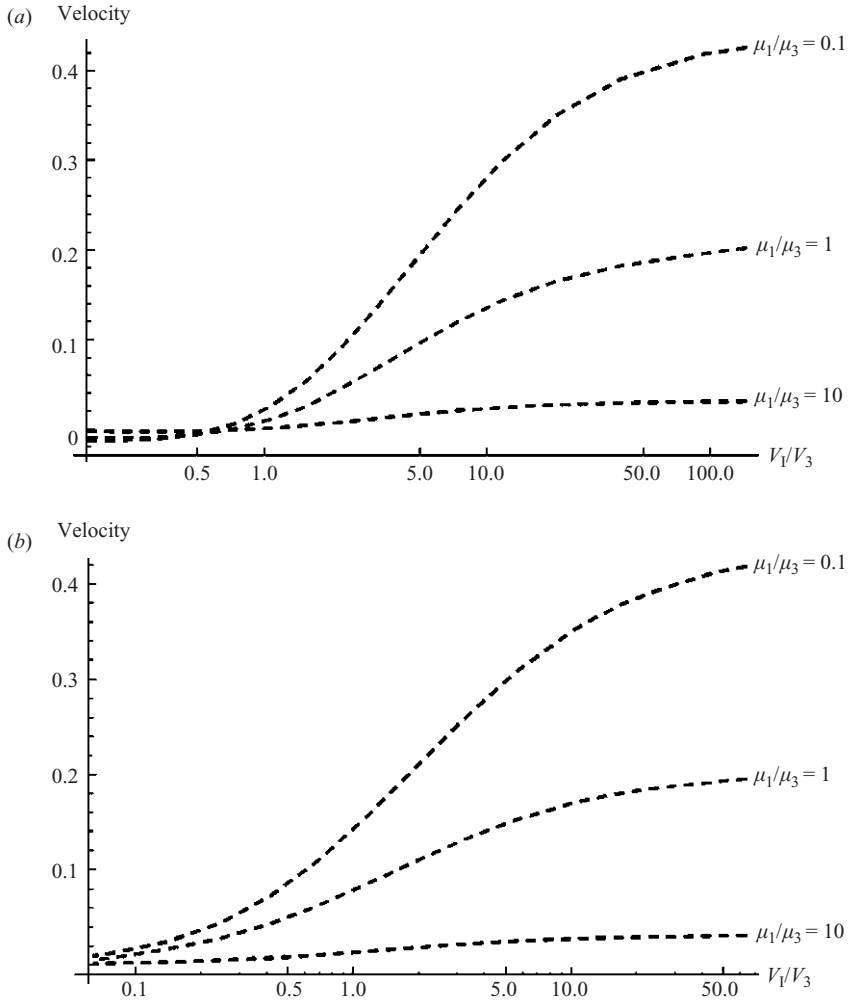

FIGURE 5. Velocity versus volume ratio for various viscosity ratios of the dispersed phases for the case of partially conducting compound drop with the lower interface (Γ_{23}) thermally inert. $\gamma_T = 1$ on all other interfaces; $\kappa_1 = 0$, $\kappa_3 = \kappa_2 = 1$; $\mu_2 = \mu_3 = 1$. The contact angles are (*a*) $\theta_1 = 0.8722\pi$, $\theta_2 = 0.95\pi$, $\theta_3 = 0.1778\pi$; (*b*) $\theta_1 = 1.02\pi$, $\theta_2 = 0.5\pi$, $\theta_3 = 0.48\pi$.

It is therefore clear that the motion of the drop against the temperature gradient depends on the drop's configuration (note once more the differences in the drop configuration for the two choices of contact angles that are qualitatively depicted in figure 3). This dependence (direction of motion on the configuration of the compound drop) is demonstrated in figures 6(*a*) and 6(*b*) in which the velocity versus volume ratio is presented for various configurations of the compound drop. It can be seen in figure 6 that, with the increase of the outer contact angle (θ_2) and as a consequence the decrease of θ_3, the drop changes its direction of motion at a certain volume ratio. For outer contact angles $\theta_2 \leqslant 0.6\pi$ the compound drop will move in the direction of the temperature gradient for any volume ratio. In figure 6(*b*), the inner angle θ_1 was kept constant at 0.5π while the other two angles were changed, respectively. Here too it can be observed that, as the value of the outer angle θ_2 decreases below 0.95π and

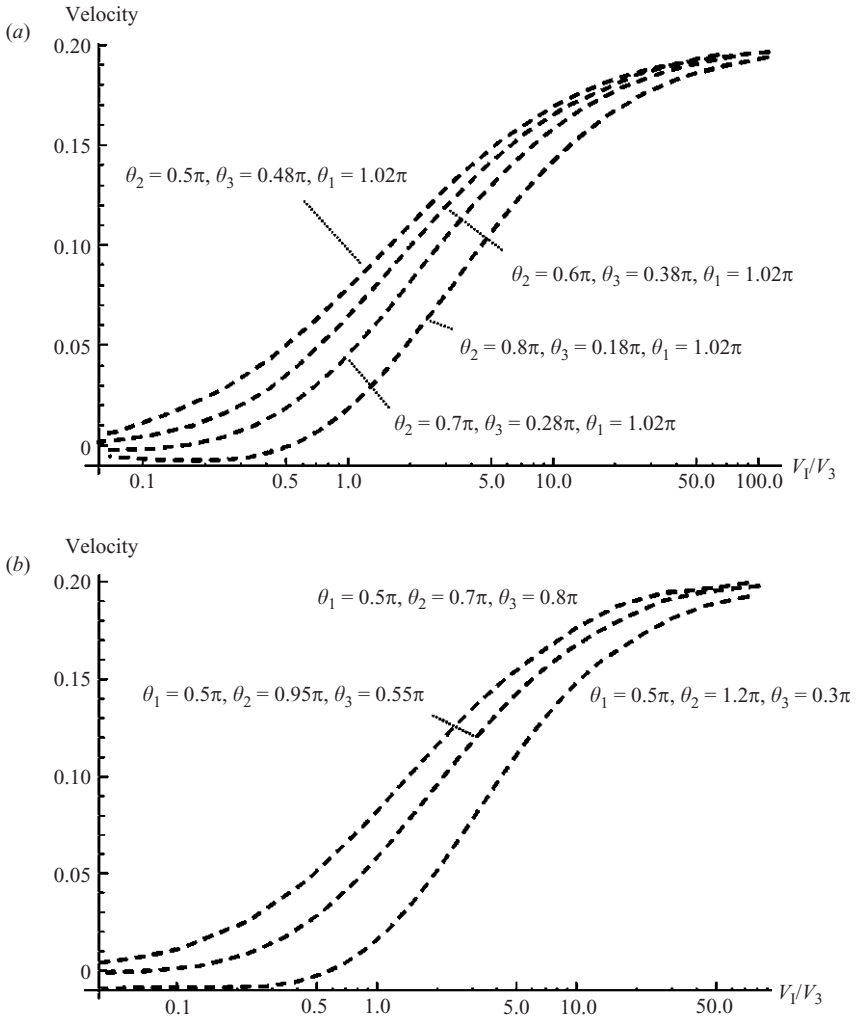

FIGURE 6. Velocity versus volume ratio for various configurations of the compound drop for the case of partially conducting drop with the lower interface (Γ_{23}) thermally inert. $\gamma_T = 1$ on all other interfaces; $\kappa_1 = 0$, $\kappa_3 = \kappa_2 = 1$; $\mu_2 = \mu_3 = 1$.

as a consequence the value of the angle θ_3 increases, the compound drop will move in the direction of the temperature gradient for any volume ratio.

The values of the velocity in the direction opposite to the temperature gradient presented in figure 6 are relatively small. Nevertheless, they are consistent with the results depicted in figures 8 and 9 (all evident at low V_1/V_3) where the velocity in the direction opposite to the thermal gradient has higher values, of the order of those obtained for the co-directional motion. Indeed, this phenomenon and its intensity can be affected by other effects such as deformability of the interfaces, inertia or convective heat transfer, that remain yet to be considered in future studies. A brief discussion of possible experimental validation of the results is given in the § 6.

It is interesting to compare between the various cases described above and those in Rosenfeld *et al.* (2008). Compound drop with equal conductivities, non-conducting compound drop and partially conducting compound drop with the sub-cases of a

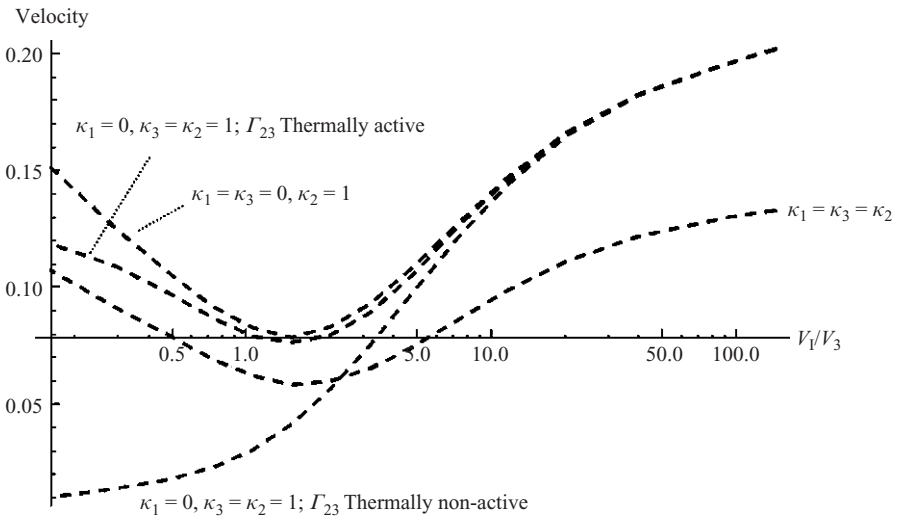

FIGURE 7. A comparison between the cases of equal conductivities, non-conductive drop and partially conducting drop with the lower interface thermally active and inert; $\theta_1 = 0.8722\pi$, $\theta_2 = 0.95\pi$, $\theta_3 = 0.1778\pi$; $\mu_1 = \mu_2 = \mu_3 = 1$; $\gamma_T = 1$ on all interfaces.

lower interface thermally active and inert, respectively. This comparison is presented in figure 7. Note that all three cases, in which phase 1 is non-conductive, approach a common asymptote when the volume of this phase is dominant. In the other extreme a greater variation in the migration velocity is observed when V_1/V_3 diminishes. When phase 1 is conducting it is expected that the high volume ratio asymptote varies as well.

It is clear from the various cases described above that the relative intensity of the variation of the various surface tensions with temperature plays an important role in dictating the dynamics of the compound drop. In certain cases, even reversal of the direction of motion of the drop is evident. It was shown in figure 5(*b*) that for the specific drops' configuration of $\theta_1 = 1.02\pi$, $\theta_2 = 0.5\pi$, $\theta_3 = 0.48\pi$ and when the lower interface (Γ_{23}) is thermally inert the drop does not change its direction of motion even for very small values of the volume ratio. It can further be noticed in figure 4 that when the lower interface (Γ_{23}) is thermally active, the compound drop does not change its direction of motion. In order to study the effect of relative 'thermal activity' of the interfaces we define a parameter G_D as the ratio of the derivative of the external tensions with temperature to the inner one, $G_D^{(12)} = \gamma_T^{(12)}/\gamma_T^{(13)}$, $G_D^{(23)} = \gamma_T^{(23)}/\gamma_T^{(13)}$, $\gamma_T^{(ij)} = \partial\gamma_{ij}/\partial T$, $\gamma_T^{(13)} = 1$, where, for the case in which the lower interface is thermally inert $G_D^{(23)} = 0$. In figures 8 and 9, the migration velocity is plotted against the volume ratio for various values of $G_D^{(ij)}$ with the viscosity of all phases being uniform for the two cases (the lower interface thermally inert and thermally active). The case in which the lower interface is thermally inert is presented in figure 8. For the particular choice of contact angles, $\theta_1 = 1.02\pi$, $\theta_2 = 0.5\pi$, $\theta_3 = 0.48\pi$, and when the temperature dependence of the interfacial tension of the external surface (Γ_{12}) is negligible ($G_D^{(12)} = 0$) a migration velocity against the temperature gradient is evident spanning a significant range of the dispersed phase volume ratio. This range diminishes as $G_D^{(12)}$increases but the negative migration velocity persists up to a ratio of about $G_D^{(12)} = 0.1$. The second case

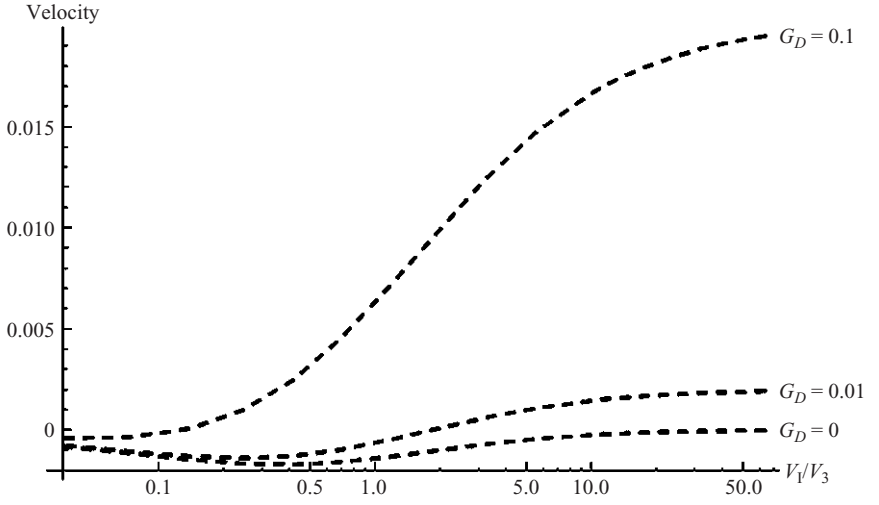

FIGURE 8. Velocity versus volume ratio for various ratios of tension temperature dependence for the case of partially conductive compound drops with the lower interface thermally inert; $\theta_1 = 1.02\pi$, $\theta_2 = 0.5\pi$, $\theta_3 = 0.48\pi$; $\kappa_1 = 0$, $\kappa_2 = \kappa_3 = 1$; $\mu_1 = \mu_2 = \mu_3 = 1$; $G_D = \gamma_T^{(12)}/\gamma_T^{(13)}$, $\gamma_T^{(13)} = 1$.

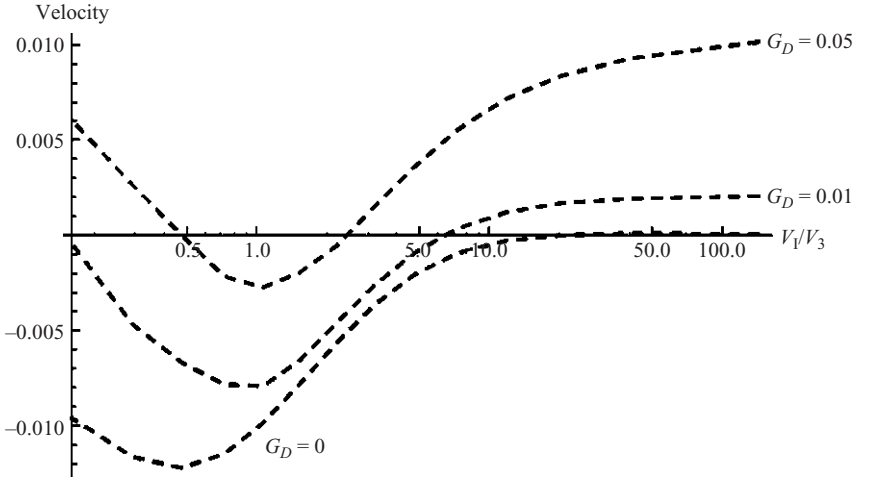

FIGURE 9. Velocity versus volume ratio for various ratios of tension temperature dependence for the case of partially conductive compound drops with the lower interface thermally active; $\theta_1 = 0.8722\pi$, $\theta_2 = 0.95\pi$, $\theta_3 = 0.1778\pi$; $\kappa_1 = 0$, $\kappa_2 = \kappa_3 = 1$; $\mu_1 = \mu_2 = \mu_3 = 1$; $G_D = \gamma_T^{(12)}/\gamma_T^{(13)} = \gamma_T^{(23)}/\gamma_T^{(13)}$, $\gamma_T^{(13)} = 1$.

in which the lower interface is thermally active, $G_D^{(12)} = G_D^{(23)}$, is presented in figure 9. It can be seen that a migration velocity against the temperature gradient is observed for a significant range of $G_D^{(ij)}$. Note that when the domain of negative velocity first appears it is confined to a volume ratio interval of $O(1)$. This interval is increased as the value of $G_D^{(23)} = G_D^{(12)}$ decreases.

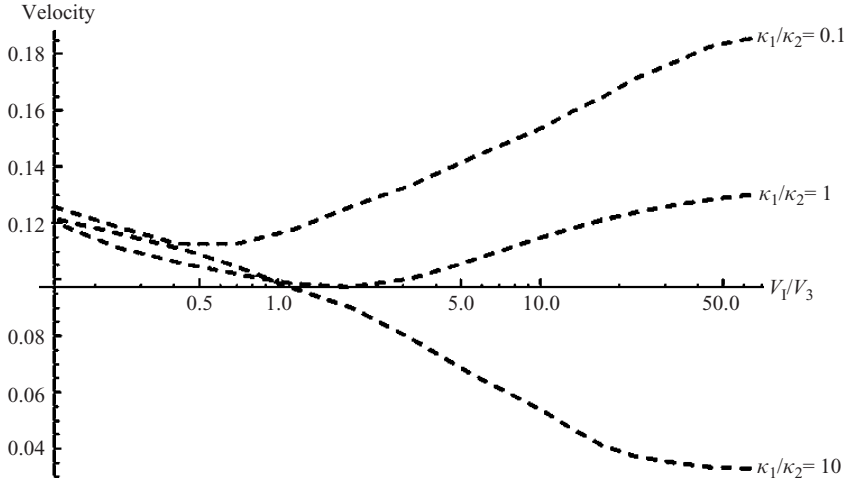

FIGURE 10. Velocity versus volume ratio for various conductivity ratios; $\theta_1 = 1.02\pi$, $\theta_2 = 0.5\pi$, $\theta_3 = 0.48\pi$; $\mu_1 = \mu_2 = \mu_3 = 1$; $\kappa_2 = \kappa_3 = 1$; $\gamma_T = 1$ on all interfaces.

5.3. *The effect of conductivity ratio*

In this subsection, we examine the effect of conductivity ratio on the dynamics of the drop. For simplicity we consider the less cumbersome case in which the upper part of the drop is spherical while the shape of lower part varies, and with $\kappa_2 = \kappa_3$ while κ_1 is arbitrary. The results are depicted in figure 10. It can be seen that when the thermal conductivity of phase 1 is much lower than that of phase 2 (and 3), the compound drop behaves as a partially conductive drop and when $V_1/V_3 \to \infty$ its velocity approaches the value of the velocity of a non-conductive drop moving under the influence of an external temperature gradient. On the other hand, when the thermal conductivity of phase 1 is much higher than that of the other phases the temperature at the interface of the upper phase is almost uniform and hence when $V_1/V_3 \to \infty$ the velocity decreases to zero since there is no driving force for the motion of the compound drop. In all the cases the migration velocity approaches the limit of a single phase conducting drop (with $\kappa_2 = \kappa_3$) as $V_1/V_3 \to 0$. Note also that when V_1/V_3 is large the velocity decays with increasing κ_1/κ_3 while when V_1/V_3 diminishes this behaviour is reversed.

5.4. *Spontaneous thermocapillary motion*

Spontaneous thermocapillary motion occurs when the system is not in thermodynamic equilibrium between the drop phases or with the ambient fluid. Heat transfer that occurs between the phases in such systems induces non-homogeneous temperature field that causes surface tension gradients and, hence, the thermocapillary migration of the compound drop is expected. For an illustration, we consider the case in which phase 1 is assumed to have constant temperature different from that of phases 2 and 3. This situation can be facilitated by assuming a large heat capacity in phase 1 with $\kappa_1 \to \infty$. Thus, to a first approximation the temperature at the interfaces Γ_{12} and Γ_{13} is uniform, T_S. The heat conducts from these surfaces towards Γ_{23} and hence causes a non-uniform temperature distribution on the latter and the motion of the entire compound drop due to the Marangoni effect. Figure 11 presents the velocity of the compound drop versus the volume ratio with viscosity ratio as a parameter for two choices of contact angles. It can be seen that for the limit of $V_1/V_3 \to \infty$, when the

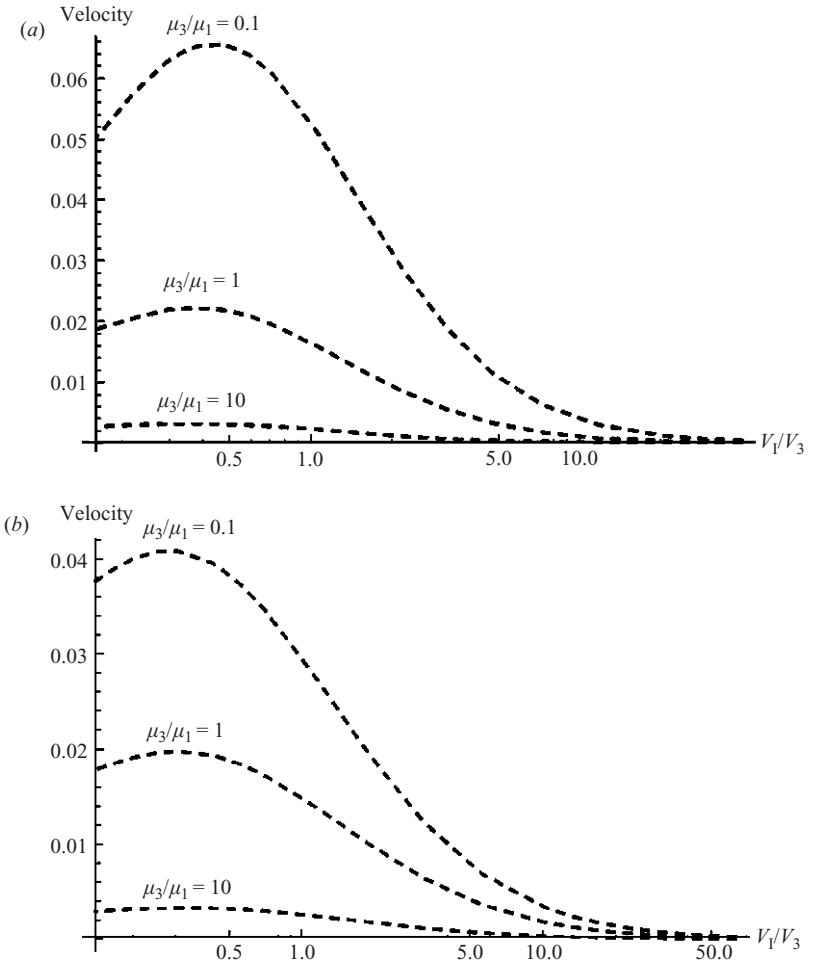

FIGURE 11. Velocity versus volume ratio for various values of the viscosity ratio; $\mu_1 = \mu_2 = 1; \kappa_2 = \kappa_3 = 1$. The contact angles are (*a*) $\theta_1 = 0.8722\pi$, $\theta_2 = 0.95\pi$, $\theta_3 = 0.1778\pi$; (*b*) $\theta_1 = 1.02\pi$, $\theta_2 = 0.5\pi$, $\theta_3 = 0.48\pi$.

drop is comprised mostly of phase 1 which is of uniform temperature, and hence no Marangoni effect is expected, the velocity approached zero with the diminishing of the driving force for its motion. Moreover, the velocity decays also at the limit $V_1/V_3 \to 0$ and hence it obtains a maximum value at a certain volume ratio in which the heat transfer between the two dispersed phases is the most efficient to induce dynamics. A comparison between the two figures reveals that the location of this maximum depends on the choice of contact angles and more weakly on the viscosity ratio between the phases of the compound drop.

The temperature distribution at the Γ_{23} interface, at which the thermocapillary motion is induced, is depicted in figure 12. The temperature is plotted versus the coordinate ξ (see figure 15) for several values of the volume ratio (V_1/V_3). When $V_1/V_3 \to \infty$ the temperature distribution at the interface is almost constant and hence, as was demonstrated in figures 11(*a*) and 11(*b*), the velocity of the compound drop diminishes. The middle curve ($V_1/V_3 \sim 1$) represents the case in which the heat transfer

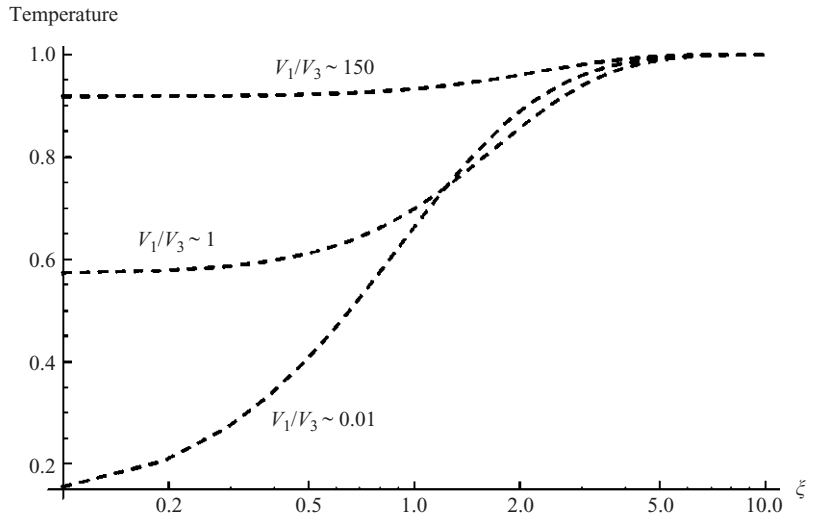

FIGURE 12. Temperature distribution at the lower interface Γ_{23} versus the coordinate ξ for various values of the volume ratio between the dispersed phases. $\theta_1 = 0.8722\pi$, $\theta_2 = 0.95\pi$, $\theta_3 = 0.1778\pi$; $\mu_1 = \mu_2 = \mu_3 = 1$; $\kappa_2 = \kappa_3 = 1$.

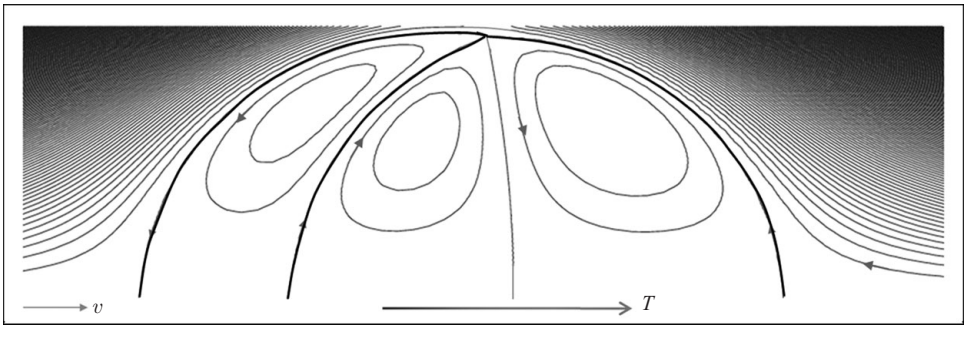

FIGURE 13. Streamlines pattern of the compound drop, moving with temperature gradient; $\kappa_1 = \kappa_2 = \kappa_3$; $G_D = 1$; $\theta_1 = 0.8722\pi$, $\theta_2 = 0.95\pi$, $\theta_3 = 0.1778\pi$; $\mu_1 = \mu_2 = \mu_3 = 1$; $V_1/V_3 = 2$.

between the phases is the most efficient. The efficiency of the heat transfer decays as the volume ratio decreases, as phase 1 becomes less pronounced.

5.5. *Flow fields*

Flow streamlines in the reference frame linked to the drop are presented in figures 13 and 14 for the two cases, motion with temperature gradient and motion against it, respectively. Several vortices are evident in the flow inside compound drop. In the depicted case a single vortex appears in fluid 3 while a double vortex is seen in fluid 1 indicating the existence of three stagnant rings within the drop and the appearance of the stream function $\Psi = 0$ within fluid 1 in addition to the interfaces. It can be seen that, in both cases, the separation line inside phase 1 is curved in the direction of motion. When the drop moves towards the hotter region (with the temperature gradient), it is directed upwards, and when the drop changes its direction of motion and starts to move to the opposite direction the line is curved against the temperature gradient.

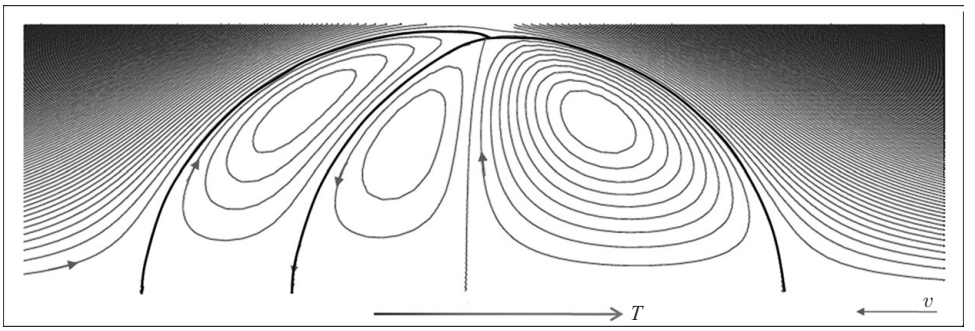

FIGURE 14. Streamlines pattern of the compound drop, moving against temperature gradient; $\kappa_1 = \kappa_2 = \kappa_3$; $G_D = 0$; $\theta_1 = 0.8722\pi$, $\theta_2 = 0.95\pi$, $\theta_3 = 0.1778\pi$; $\mu_1 = \mu_2 = \mu_3 = 1$; $V_1/V_3 = 2$.

6. Further discussion and conclusions

In this manuscript an analytical method was developed in order to study the motion of a compound multiphase drop under the influence of an external temperature gradient as well as the spontaneous thermocapillary motion of such a drop. In both cases the inhomogeneous distribution of temperature at the hybrid drops' interfaces results in surface tension variations which, in turn, induce Marangoni-type flow and migration of the fluid particle. The case of the motion of a compound drop due to an external temperature gradient was considered for following three limiting cases:

(i) Non-conducting compound drop. In this case it was shown that the velocity approaches that of a non-conducting compound bubble when the compound drop is comprised of mostly non-viscous phase and it approaches the velocity of a non-conducting nearly solid particle when the drop is comprised of mostly a highly viscous fluid.

(ii) Partially conducting compound drop. Here it was shown that when the lower interface (Γ_{23}) is not thermally active and when the drop is comprised mostly of non-viscous phase, the drop changes its direction of motion and moves against the direction of the temperature gradient. This occurs since in that case the motion is driven mostly by tension variations at the interface which separates the two phases comprising the drop (Γ_{13}). It was further shown that this phenomenon occurs for several specific configurations (contact angles) of the compound drop while for other configurations it cannot be observed. When the lower interface (Γ_{23}) is thermally active, the values of the velocity approach the value of a non-conductive single bubble when the drop is comprised mostly of non-viscous non-conductive phase and it approaches the value of the velocity of a conductive solid particle when the drop is comprised of a highly viscous conductive phase. The phenomenon of motion against the temperature gradient can be observed here as well in case when the motion of the inner interface (Γ_{13}) due to surface tension variations becomes the major driving force for the motion of the entire compound drop. These results can be highly useful since it was shown that there is a control mechanism in which one is able to control the direction of motion of the compound drop.

(iii) Compound drop comprised of a full sphere and an attached spherical segment. Here we have studied the influence of the conductivity ratio on the motion of the compound drop. It was shown that when the thermal conductivity of the upper phase (phase 1) is much lower than that of the other two phases the velocity of the drop approaches the velocity of a partially conductive drop and when the drop is comprised of mostly phase 1 the value approaches that of a non-conductive liquid

sphere moving under the influence of an external temperature gradient. On the other hand when the thermal conductivity of phase 1 is much higher than that of the other phases and for a compound drop comprised of mostly phase 1 the velocity decreases to zero since, in this case, the driving force for the motion of the drop is diminished.

In most cases where the motion induced by an external temperature field the velocity of the compound drop exhibits a minimum when respective volumes of the drop phases are nearly equal. The velocity of this configuration is much smaller than the respective asymptotes of $V_1/V_3 \to 0$ and $V_1/V_3 \to \infty$ suggesting that $V_1/V_3 \sim O(1)$ represents a compound drop with a relatively high resistance to motion.

Investigation of the case of spontaneous thermocapillary motion of a compound drop revealed that the drop can migrate due to interfacial heat flux between the phases. It was shown that when the drop is comprised mostly of the upper phase (phase 1) and with $\kappa_1 \to \infty$ the value of the velocity approaches zero since the temperature at the interface of that phase is uniform. Moreover, the velocity value obtains a maximum at a certain drops' configuration in which the variation of tension due to the heat transfer is most pronounced. The location of this maximum value changes with each configuration of the compound drop.

The results of the research should be useful for a better understanding of the role of the Marangoni effect in natural and technological processes involving multiphase flows with a changing topology of the dispersed phases such as emulsification, liquid–liquid extraction, composite material processing, etc.

The analysis in this paper is restricted to the motion induced solely by the Marangoni effect in the absence of other external forcing. The motion of a partially engulfed compound drop induced solely by gravity and buoyancy was studied by Oğuz (1987) and Vuong & Sadhal (1989*a*). Their derivations were revisited also in our recent paper (Rosenfeld *et al.* 2008). Due to the linearity of the problem, the velocity of a partially engulfed drop moving under the simultaneous effect of gravity and thermocapillarity can be obtained by a simple superposition of the two results. The physical results are anticipated to be similar to those obtained for a single-phase drop (see, e.g. Young *et al.* 1959), e.g. an upward temperature gradient will hinder gravitational sedimentation of a heavy drop and, at a critical magnitude of this gradient, the gravity and thermocapillary forces will be balanced halting the drop motion. These phenomena can probably be observed in experiments similar to those conducted by Young *et al.* (1959). In such experiments it can be anticipated that the deformations of the interfaces will differ from those in the case of a single-phase drop, since the variation of the temperature, as the drop propagates to hotter regions, alters the contact angles in addition to the effect on the three interfaces.

No experiments concerning the thermocapillary motion of partially engulfed drops are available so far. We believe that the motion in the direction of temperature gradient can be observed for the compound drops used previously in the experiments by Mercier *et al.* (1974), Mori *et al.* (1977), Mori (1978) and Hashimoto & Kawano (1990) adapting the classical experimental technique of Young *et al.* (1959). Observation of the motion in the direction opposite to that of the temperature gradient might be a more complicated task, since this phenomenon takes place when the inner interface is substantially more thermocapillary active than the outer ones, i.e. the dependence of the interfacial tension on temperature there is considerably stronger than at the outer interfaces. Thus, such experiments require a very careful choice of the three phases involved. Additional discussion of the subject is given in Rosenfeld *et al.* (2008).

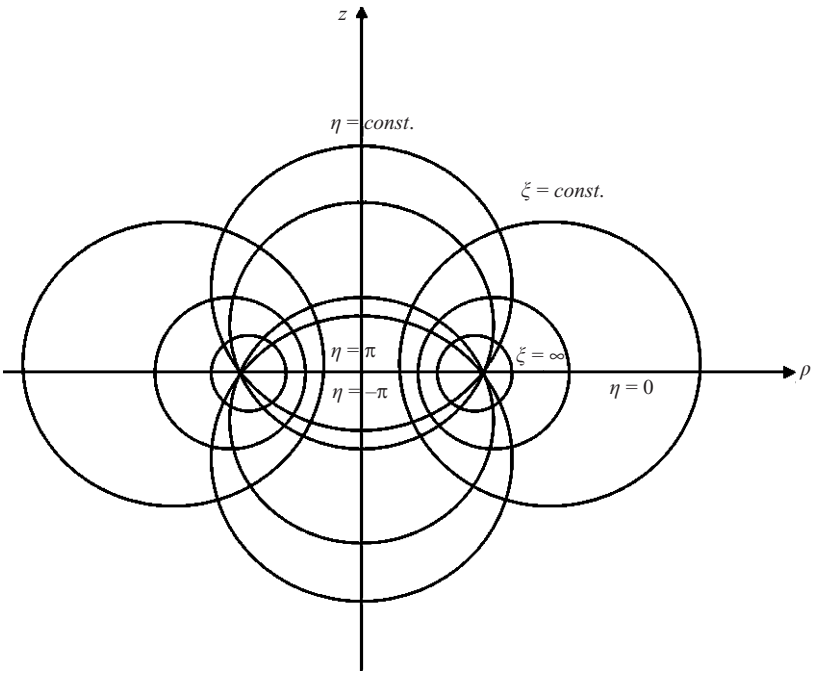

FIGURE 15. The toroidal coordinate system.

This research was supported in part by the Asher Space Research Institute at the Technion. O. M. Lavrenteva acknowledges the support of the Israel Ministry for Immigrant Absorption.

Appendix A. Stream function in toroidal coordinates

The stream function ψ satisfies

$$L_{-1}^2\psi = 0, \tag{A 1}$$

where L_{-1} is the axisymmetric Stokes operator. In a cylindrical coordinate system (ρ, z), it can be written as

$$L_{-1} = \frac{\partial^2}{\partial\rho^2} - \frac{1}{\rho}\frac{\partial}{\partial\rho} + \frac{\partial^2}{\partial z^2}. \tag{A 2}$$

Since the interfaces of the drop are assumed to be of uniform curvatures, following Vuong & Sadhal (1989*a*, *b*), it is beneficial to employ the toroidal coordinate system (ξ, η) related to the cylindrical system by

$$z + i\rho = ic\ \coth\frac{\xi + i\eta}{2}, \quad 0 \leqslant \xi < \infty, \quad -\pi \leqslant \eta \leqslant \pi \tag{A 3}$$

The toroidal coordinate system is presented in figure 15. It can be seen that constant values of η represents intersecting spherical segments. Here the interface Γ_{ij} is identified by η_{ij}, c is the distance between the origin and the focal circle defined by $\xi = \infty$ which, in the compound drop, is the three-phase boundary. The real value

components of the above mapping have the following form:

$$\rho = \frac{c \sinh \xi}{\cosh \xi - \cos \eta}, \quad z = \frac{c \sin \eta}{\cosh \xi - \cos \eta}. \tag{A 4}$$

The velocity components are given by

$$(u_\xi, u_\eta) = \frac{(\cosh \xi - \cos \eta)^2}{c^2 \sinh \xi} \left(\frac{\partial \psi}{\partial \eta}, -\frac{\partial \psi}{\partial \xi} \right) \tag{A 5}$$

and the shear stress is written as

$$\sigma_{\xi\eta} = \mu \left[(\cosh \xi - \cos \eta) \left(\frac{\partial u_\xi}{\partial \eta} + \frac{\partial u_\eta}{\partial \xi} \right) + u_\xi \sin \eta + u_\eta \sinh \xi \right], \tag{A 6}$$

where, $\Psi_{uniform} = U/2(c \sinh \xi/(\cosh \xi - \cos \eta))^2$, with U scaled by U_M, and the disturbance $\Psi^{(2)} = 1/(\cosh \xi - \cos \eta)^{3/2} \int_0^\infty \phi^{(2)}(\eta, \lambda) \sinh^2 \xi P'_{-1/2+i\lambda}(\cosh \xi) \mathrm{d}\lambda$.

Following Payne & Pell (1960) and Voung & Sadhal (1989*a*) we combine these two functions together to get

$$\begin{aligned} \phi^{(2)}_{total} = UN(\eta, \lambda) &+ \cos \eta [A^{(2)}(\lambda) \cosh \lambda\eta + B^{(2)}(\lambda) \sinh \lambda\eta] \\ &+ \sin \eta [C^{(2)}(\lambda) \cosh \lambda\eta + D^{(2)}(\lambda) \sinh \lambda\eta]. \end{aligned} \tag{A 7}$$

In this expression, $N(\eta, \lambda)$ appears from the expansion

$$\frac{1}{2} \left[1 - \frac{c}{r} \right] = (\cosh \xi - \cos \eta)^{1/2} \int_0^\infty N(\eta, \lambda) P'_{-1/2+i\lambda}(\cosh \xi) \, \mathrm{d}\lambda \tag{A 8}$$

with $r = \sqrt{\rho^2 + z^2}$ and where the first term on the left-hand side arises from the uniform stream and the second term is subtracted in order to render the integrals readily convergent. Thus the function $N(\eta, \lambda)$ is found to be (Vuong & Sadhal 1989*a*)

$$N(\eta, \lambda) = \frac{\lambda \sin |\eta| (\sinh \lambda|\eta| - \sinh \lambda(\pi - |\eta|))}{\sqrt{2}(\lambda^2 + 1) \cosh \lambda\pi} - \frac{\cos \eta (\cosh \lambda(\pi - |\eta|) + \cosh \lambda\eta)}{\sqrt{2}(\lambda^2 + 1) \cosh \lambda\pi}. \tag{A 9}$$

Note that the jump in the coordinate η, described schematically in figure 15, is located within one of the fluid phases. When applying the boundary conditions it should prove useful to move the domain cut to one of the interfaces and render the application less cumbersome. We have chosen to cut the domain at the inner interface which means that the surface coordinate is now $\eta_{13} + 2\pi$ in phase 1 and η_{13} in phase 3.

Substituting the presentations of the stream function into the boundary conditions provides 12 linear algebraic equations for the coefficients $A^{(i)}(\lambda)$, $B^{(i)}(\lambda)$, $C^{(i)}(\lambda)$, $D^{(i)}(\lambda)$ in the three phases that, thus, can be obtained in an explicit analytic form for an arbitrary migration velocity U_∞ and arbitrary right-hand side of (2.6). These explicit expressions obtained employing Mathematica are available from the authors upon request.

For the thermocapillary motion, the stream function coefficients consist of two additive parts. One is due to the thermocapillary traction at the interfaces, while another is proportional to the yet unknown migration velocity. Note that the coefficients $A^{(i)}(\lambda)$, $B^{(i)}(\lambda)$, $C^{(i)}(\lambda)$, $D^{(i)}(\lambda)$ corresponding to the first part and the multipliers of U_∞ are readily known as explicit analytic expressions that do not contain any unknowns. Similarly, the force F is a sum of a Marangoni force acting on a quiescent drop and a Stokes drag proportional to U_∞. The condition of zero total

force exerted on the drop by the Stokes flow, allows to determine the migration velocity by calculating integrals of the type (3.1) and (3.5) with known integrands. As soon as the migration velocity is obtained, the stream function is obtained by integration. The required integrations were performed numerically over a finite interval $(0, L)$ making use of Mathematica 6 gradually extending the domain of integration until the desired accuracy of integration is achieved.

REFERENCES

Berejnov, V., Leshansky, A. M., Lavrenteva, O. M. & Nir, A. 2002 Spontaneous thermocapillary interaction of drops: effect of surface deformation at nonzero capillary number. *Phys. Fluids* **14**, 1326–1339.

Bialik-Rosenfeld, L., Lavrenteva, O. M. & Nir, A. 2007 Spontaneous thermocapillary drops interaction: the effect of a surface reaction. *AIChE J.* **53**, 2783–2794.

Borhan, A., Haj-Hariri, H. & Nadim, A.1992 Effect of surfactants on the thermocapillary migration of a concentric compound drop. *J. Colloid Interface Sci.* **149**, 553–560.

Dammel, F. & Beer, H. 2003 Heat transfer from a continuous liquid to an evaporating drop: a numerical analysis. *Intl J. Thermal Sci.* **42**, 677–686.

Feuillebois, F. 1989 Thermocapillary migration of two equal bubbles parallel to their line of centers. *J. Colloid Interface Sci.* **131**, 267–274.

Golovin, A. A., Nir, A. & Pismen, L. M. 1995 Spontaneous motion of two droplets caused by mass transfer. *Ind. Engng Chem. Res.* **34**, 3278–3288.

Haj-Hariri, H., Nadim, A. & Borhan, A. 1993 Reciprocal theorem for concentric compound drops in arbitrary Stokes flows. *J. Fluid Mech.* **252**, 265–277.

Hashimoto, H. & Kawano S. 1990 A study on encapsulated liquid drop formation in liquid–liquid–gas systems (fundamental mechanisms of encapsulated drop formation). *JSME Intl J. Ser. II* **33** (4), 729–735.

Johnson, R. E., & Sadhal, S. S. 1985 Fluid mechanics of compound multiphase drops and bubbles. *Annu. Rev. Fluid Mech.* **17**, 286–320.

Lavrenteva, O. M., Leshansky, A. M., Berejnov, V. & Nir, A. 2002 Spontaneous thermocapillary interaction of drops, bubbles and particles in viscous fluid driven by capillary inhomogeneties. *Ind. Engng Chem. Res.* **41**, 357–366.

Lavrenteva, O. M., Leshansky, A. M. & Nir, A. 1999 Spontaneous thermocapillary interaction of drops, bubbles and particles: unsteady convective effects at low Péclet numbers. *Phys. Fluids* **11**, 1768–1782.

Lavrenteva, O. M. & Nir, A. 2001 Spontaneous thermocapillary interaction of drops and bubbles: unsteady convective effects at high Péclet numbers. *Phys. Fluids* **13**, 368–381.

Lebedev, N. N. 1965 *Special Functions and Their Applications*. Prentice-Hall.

Loewenberg, M. & Davis, R. H. 1993*a* Near-contact thermocapillary migration of a non-conducting, viscous drop normal to a planar interface. *J. Colloid Interface Sci.* **160**, 265–274.

Loewenberg, M. & Davis, R. H. 1993*b* Near-contact thermocapillary motion of two non-conducting drops. *J. Fluid Mech.* **256**, 107–131.

Lyell, M. J. & Carpenter, M. J. 1993 The effect of residual contamination on Marangoni convection in a spherical liquid system. *Appl. Sci. Res.* **14**, 639–662.

Mercier, J. L., da Cunha, F. M., Teixeria, J. C. & Scofield M. P. 1974 Influence of enveloping water layer on the rise of air bubbles in Newtonian fluid. *J. Appl. Mech.* **96**, 29–34.

Mori, Y. H. 1978 Configurations of gas–liquid two phase bubbles in immiscible liquid media. *Int. J. Multiphase Flow* **4**, 383–396.

Mori, Y. H., Komotori, K., Higeta, K. & Inada, J. 1977 Rising behavior of air bubbles in superposed liquid layers. *Can. J. Chem. Engng* **55**, 9–12.

Morton, D. S., Subramanian, R. S. & Balasubramaniam, R. 1990 The migration of a compound drop due to thermocapillarity. *Phys. Fluids* A **2**, 2119–2133.

Oğuz, H. N. 1987 Fluid dynamics of compound multiphase drops and bubbles. Ph.D. thesis, University of Southern California.

Payne, L. E. & Pell, W. H. 1960 The Stokes flow problem for a class of axially symmetric bodies. *J. Fluid Mech.* **7**, 529–549.

Rosenfeld, L., Lavrenteva, O. M. & Nir, A. 2008 Thermocapillary motion of hybrid drops. *Phys. Fluids* **20** (7), 072102.

Sadhal, S. S. 1983 A note on the thermocapillary migration of a bubble normal to a plane surface. *J. Colloid Interface Sci.* **95**, 283–285.

Sideman, S. & Taitel, Y. 1964 Direct contact heat transfer with change of phase: evaporation of drops in an immiscible liquid medium. *Intl J. Heat Mass Transfer* **7**, 1273–1289.

Sneddon, I. N. 1972 *The Use of Integral Transforms.* McGraw-Hill.

Stone, H., & Leal. G. 1990 Breakup of concentric double emulsion droplets in linear flow. *J. Fluid Mech.* **211**, 123–156.

Subramanian, R. S. & Balasubramaniam R. 2001 *The Motion of Bubbles and Drops in Reduced Gravity*. Cambridge University Press.

Tochitani, Y., Mori, Y. H. & Komotori, K. 1977*a* Vaporizing of single drops in an immiscible liquid. Part I. Forms and motions of vaporizing drops. *Thermo Fluid Dyn.* **10**, 51–59.

Tochitani, Y., Nakagawa, T., Mori, Y. H. & Komotori, K. 1977*b* Vaporizing of single drops in an immiscible liquid. Part II. Heat transfer characteristics. *Thermo Fluid Dyn.* **10**, 71–79.

Torza, S. & Mason, S. G. 1970 Three-phase interactions in shear and electrical fields. *J. Colloid Interface Sci.* **33**, 67–83.

Tsemakh, D., Lavrenteva, O. M. & Nir, A. 2004 On the locomotion of a drop induced by the internal secretion of surfactant. *Intl J. Multiphase Flow* **30**, 1337–1367.

Vuong, S. T. & Sadhal, S. S. 1989*a* Growth and translation of a liquid–vapor compound drop in a second liquid. Part 1. Fluid mechanics. *J. Fluid Mech.* **209**, 617–637.

Vuong, S. T. & Sadhal, S. S. 1989*b* Growth and translation of a liquid–vapor compound drop in a second liquid. Part 2. Heat transfer. *J. Fluid Mech.* **209**, 639–660.

Young, N. O., Goldstein, J. S. & Block M. J. 1959 The motion of gas bubbles in a vertical temperature gradient. *J. Fluid Mech.* **6**, 350–364.

Zabarankin, M. 2007 Asymmetric three-dimensional Stokes flows about two fused equal spheres. *Proc. R. Soc.* A **463**, 2329–2349.